Monthly Notices
of the
ROYAL ASTRONOMICAL SOCIETY

Mon. Not. R. Astron. Soc. **413,** 2665–2678 (2011) doi:10.1111/j.1365-2966.2011.18335.x

Bridging the gap between low- and high-mass dwarf galaxies

Duncan A. Forbes,[1]⋆ Lee R. Spitler,[1] Alister W. Graham,[1] Caroline Foster,[1] G. K. T. Hau[1] and Andrew Benson[2]

[1]*Centre for Astrophysics & Supercomputing, Swinburne University, Hawthorn, VIC 3122, Australia*
[2]*Mail Code 350-17, California Institute of Technology, Pasadena, CA 91125, USA*

Accepted 2011 January 11. Received 2010 December 12; in original form 2010 July 23

ABSTRACT

While the dark matter content within the most-massive giant and smallest dwarf galaxies has been probed – spanning a range of over one million in mass – an important observational gap remains for galaxies of intermediate mass. This gap covers K-band magnitudes of approximately $-16 > M_K > -18$ mag (for which dwarf galaxies have $B - K \sim 2$). On the high-mass side of the gap are dwarf elliptical (dE) galaxies that are dominated by stars in their inner regions. While the low-mass side includes dwarf spheroidal (dSph) galaxies that are dark matter dominated and ultracompact dwarf (UCD) objects that are star-dominated. Evolutionary pathways across the gap have been suggested but remain largely untested because the 'gap' galaxies are faint, making dynamical measurements very challenging.

With long exposures on the Keck telescope using the Echelle Spectrograph and Imager instrument, we have succeeded in bridging this gap by measuring the dynamical mass for five dwarf galaxies with $M_K \sim -17.5$ ($M_B \sim -15.5$). With the exception of our brightest dwarf galaxy, they possess relatively flat velocity dispersion profiles of around 20 km s^{-1}. By examining their 2D scaling relations and 3D fundamental manifold, we found that the sizes and velocity dispersions of these gap galaxies reveal continuous trends from dE to dSph galaxies. We conclude that low-luminosity dE galaxies are dominated by stars, not by dark matter, within their half light radii. This finding can be understood if internal feedback processes are operating most efficiently in gap galaxies, gravitationally heating the centrally located dark matter to larger radii, whereas external environmental processes, which can strip away stars, have a greater influence on dSph galaxies, resulting in their higher dark matter fractions. UCD objects appear to be more similar to massive compact star clusters than to small galaxies. Our dynamical study of low-mass dE galaxies provides further constraints on the processes that shape some of the smallest and most-numerous galaxies in the Universe.

Key words: galaxies: dwarf – galaxies: evolution – galaxies: kinematics and dynamics – galaxies: star clusters: general.

1 INTRODUCTION

Galaxies are predicted to form within massive haloes of dark matter (DM), with the galaxy stellar mass making up only a small fraction of the total mass (e.g. Benson & Bower 2010). In order to measure the total mass of an individual galaxy and hence probe the actual fraction of dark and stellar matter, one requires a dynamical study. Such studies typically measure the motion of stars well within a projected radius containing half of the total galaxy light (called the half-light or effective radius R_e). For galaxies that are dominated by random motions in their inner regions, past dynamical studies have ranged from the most-massive elliptical galaxies to the lowest-mass dwarfs. However, a single gap exists for which no dynamical studies are currently available.

This mass gap represents a key transition region from high-mass dwarf elliptical (dE) galaxies that are stellar mass dominated in their inner regions (De Rijcke et al. 2006; Toloba et al. 2011) to dwarf spheroidal (dSph) galaxies that are DM-dominated (e.g. Wolf et al. 2010) and ultracompact dwarf (UCD) objects that are dominated by stars (Dabringhausen, Hilker & Kroupa 2008; Forbes et al. 2008; Mieske et al. 2008). These systems are all largely devoid of gas, consist of old-age stars, have smooth featureless morphologies and are pressure-supported by random internal stellar motions. The relationship between these three types of dwarf systems is a subject of active debate.

⋆E-mail: dforbes@swin.edu.au

© 2011 The Authors
Monthly Notices of the Royal Astronomical Society © 2011 RAS

Here we define the gap, somewhat subjectively, to be dwarf galaxies less massive than the lowest-mass dE studied to date (Geha, Guhathakurta & van der Marel 2003; Chilingarian 2009) and more massive than the Fornax dSph galaxy (the most massive in the Local Group). In terms of the absolute K-band magnitude, this corresponds to roughly $-16 > M_K > -18$ mag. Over this magnitude range, dEs have colours of $B - K \sim 2$ (Forbes et al. 2008). With this definition of the gap, two of the Local Group dE galaxies (i.e. NGC 147 and 185) lie within the gap.

Despite being numerous in the Universe, our Local Group of galaxies contains only three dEs. All three have been classified as peculiar due to their ongoing interaction with the Andromeda galaxy, which may influence their measured dynamical mass (De Rijcke et al. 2006). They may therefore be atypical examples of their class. We must look further afield for samples of dEs that are not tidally interacting with a larger galaxy. However, beyond the Local Group, such galaxies are of low surface brightness making it very challenging for current telescopes to measure the internal motions of their stars.

The Local Group contains two dozen dSph galaxies. Although of lower luminosity than dEs, these dSph galaxies are sufficiently close to measure their velocity dispersions (from individual stars). They are all located within, or nearby to, the haloes of the giant Milky Way and Andromeda galaxies. Many of them reveal an elongated asymmetric structure indicative of an ongoing tidal interaction.

Several different formation processes have been suggested for the origin of dE and dSph galaxies. These include: (i) a *cosmological* origin in which the dwarfs are formed in the early universe. Although many will be accreted as the basic building blocks of larger galaxies and some will merge with other dwarfs, a fraction of the original population may survive until today (Nagashima et al. 2005; Valcke, De Rijcke & Dejonghe 2008; Bovill & Ricotti 2009); (ii) *environmental* processes that modify the structure of a larger progenitor galaxy. Here tidal interactions (Moore et al. 1996; Mastropietro et al. 2005; Mayer et al. 2007; D'Onghia et al. 2009) remove stellar and DM, while the so-called 'ram pressure' stripping can remove any gas (Peñarubbia, Navarro & McConnachie 2008; Mayer et al. 2010); and (iii) gravitational collapse of dense *tidal* material that was left over from the collision of large galaxies (Okazaki & Taniguchi 2000). As dwarf galaxies appear to be a heterogeneous class of objects, multiple origins may be required to explain their properties (see review by Lisker 2009).

The known UCDs are mostly located outside the Local Group, in the Virgo, Fornax and Coma clusters of galaxies. They have similar *stellar* masses and luminosities to dSph galaxies but they are more compact. There is an ongoing debate as to whether UCDs were originally the nuclei of larger dwarf galaxies or are simply massive compact star clusters (Dabringhausen et al. 2008; Forbes et al. 2008; Mieske et al. 2008). In the former scenario, UCDs are the remnant of a nucleated dE galaxy that has lost its outer stars due to tidal stripping (Bekki, Couch & Drinkwater 2001), leaving only a nuclear star cluster which is subsequently identified as an UCD.

A key discriminant between the different origins for dwarfs is their predicted DM content. Cosmological models involving cold DM robustly predict high densities of DM at the centres of dwarf galaxies (e.g. Navarro et al. 2004). However, the introduction of the energy feedback from supernova explosions in hydrodynamical models that incorporate stars and gas shows that gravitational heating causes the DM to expand to larger radii resulting in shallower DM profiles (Mashchenko, Wadsley & Couchman 2008; Romano-Diaz et al. 2008; Governato et al. 2010). These models can produce a dwarf galaxy with equal fractions of stars and DM within the effective radius. Simulations of galaxies that are subject to vigorous tidal and ram pressure stripping produce low-mass, gas-free dE and dSph galaxies with a high DM fraction in their inner regions (Mayer et al. 2001). If dwarf galaxies had their origin in the tidal material left over from a major collision, then it is expected that they would be star-dominated, containing little or no DM (Okazaki & Taniguchi 2000). We note that the simulated tidal dwarf galaxy (model RS1-5) of Kroupa (1997) has an effective radius of 180 pc, velocity dispersion of 2.8 km s^{-1} and an inferred total-to-stellar mass of >100 (i.e. similar to the inferred properties of dSph galaxies) and yet it is DM-free. Simulations by Goerdt et al. (2008) suggest that an UCD formed by the tidal stripping of a nucleated galaxy will be DM-dominated. This is in contrast to the star cluster origin for UCDs in which they will be DM-free like globular clusters (GCs) (Moore 1996; Conroy, Loeb & Spergel 2010; Lane et al. 2010).

The abundances, luminosities and, particularly, the masses of dwarf galaxies can place a strong constraint on models of galaxy formation as dwarf galaxies are highly sensitive to the details of feedback processes (e.g. Benson et al. 2002) due to their shallow potential wells. This makes them a key population which any plausible model of galaxy formation must explain. The masses and DM content of dwarf galaxies in the gap ($-16 > M_K > -18$ mag) and hence the relative role of feedback and external environmental processes are currently unknown. In particular, it is unknown if these galaxies will show a smooth transition in their dynamical properties from dEs to dSphs or to UCDs as we traverse from the high- to the low-mass side of the gap.

Here we present new measurements of the velocity dispersion of dE galaxies that lie within the gap using long exposures on the Keck 10-m telescope. With these data we derive their dynamical masses using the technique of Wolf et al. (2010) that is robust to the 3D orbits of the dynamical tracer stars. Our dynamical mass gives the total mass of stars, gas and DM within the 3D half-light radius. It allows us to constrain the fraction of DM within the inner regions of galaxies that occupy the gap region and to compare their properties to other dwarf systems for the first time.

2 SAMPLE SELECTION

We selected dE galaxies with K-band magnitudes to lie within or close to the 'gap' reported by Forbes et al. (2008). These galaxies were further constrained to have no nucleus (dE) or only a small nuclear (dE,N) component as a nuclear cluster will have its own dynamical properties distinct from the underlying galaxy (Carter & Sadler 1990; Geha, Guhathakurta & van der Marel 2002; Geha et al. 2003).

A total of five dE galaxies in the NGC 1407 and Leo groups, and Virgo cluster were chosen for observation over a single night. The basic properties of the sample galaxies are listed in Table 1.

3 DATA ACQUISITION

The five dE galaxies were observed using the Echelle Spectrograph and Imager (ESI) on the Keck II 10-m telescope on the night of 2010 January 10. Conditions were clear with typical seeing for the science exposures of 0.8 arcsec. Each galaxy was observed in high-resolution ($R \sim 20\,000$) echelle mode giving a useful wavelength range of ~4000 to 10 000 Å. The pixel-scale varies from 0.12 arcsec pixel^{-1} in the blue to 0.17 arcsec pixel^{-1} in the red across the 10 echelle orders. The slit width was 0.5 arcsec giving an instrument resolution of $\sigma = 15.8$ km s^{-1} (although we can measure

Table 1. Dwarf galaxy sample properties.

Galaxy name	Type	Distance (Mpc)	K (mag)	M_K (mag)	R_e (arcsec)	R_e (pc)
LEDA 074886	dE	25	12.21	−19.79	∼9	1130
PGC 032348	dE,N	11	13.18	−17.04	11.9	638
VCC 1826	dE,N	16.5	13.50	−17.59	6.78	542
VCC 1407	dE,N	16.5	12.41	−18.68	11.27	902
VCC 846	E?	16.5	*	−17.84	12.74	1019

Notes. Galaxy types are from the NED. The distance sources are LEDA 074886 (Trentham, Tully & Mahdavi 2006), PGC 032348 (Trentham & Tully 2002) and VCC objects (Mei et al. 2007). The K-band magnitudes are from the Two-Micron All-Sky Survey (2MASS) (*no K-band available, used $M_g = -15.34$ mag from Janz & Lisker 2009 and assumed $g - K = 2.5$, see Section 8.1 for details). The geometric mean effective radii for the VCC galaxies are from Sérsic fits to surface brightness profiles from Janz & Lisker (2008); otherwise, radii are measured in this work.

Table 2. Observing parameters.

Galaxy name	Exposure time (min)	Seeing (arcsec)	PA (°)	S/N
LEDA 074886	$20 \times 7 = 140$	0.75	103	20
PGC 032348	$25 \times 4 = 100$	0.80	65	15
VCC 1826	$20 \times 3 = 60$	0.75	−225	25
VCC 1407	$23 \times 3 = 69$	0.85	−225	20
VCC 846	$30 \times 5 = 150$	0.80	−208	5

Notes. S/N is the typical signal-to-noise ratio in the continuum at ∼8500 Å.

velocity dispersions of about half this value). The slit length is 20 arcsec and each galaxy was offset from the centre of the slit by about 5 arcsec, giving increased radial coverage in one direction. Multiple exposures were taken of each galaxy, details of which are summarized in Table 2, along with the seeing conditions and the position angle of the slit. The position angles were chosen to match that of the galaxy major-axis, if available; otherwise, a parallactic angle was used. The continuum signal-to-noise ratio (S/N) in order 9 (∼8500 Å) is also listed in Table 2. We also obtained spectra for a K giant with the same instrument settings as the science data.

Images in the B and R bands were also taken with the ESI of the Leo group dwarf galaxy PGC 032348. The pixel-scale for imaging is 0.15 arcsec pixel^{-1}. The total exposure times were 240 s in B and 120 s in R, with seeing conditions of ∼1 arcsec. Digitized Sky Survey (DSS) images of the five galaxies and the slit positions are shown in Fig. 1.

3.1 Data reduction

After checking for consistency, individual calibration files such as bias frames, HgXe and CuAr arcs, and internal flat-fields were combined to create master files. The science frames, each of the same exposure time, were average combined in 2D using the IRAF software package. The individual science frames did not require shifting as the spatial alignment of the spectra was within 1 pixel from frame to frame. An average σ clipping was used to reject cosmic rays.

Tracing and rectifying the spectra, wavelength calibration, extraction of 1D spectra in various apertures and background sky subtraction were all performed using the MAKEE program written by T. Barlow. The trace was carried out using a K giant standard star and gave residuals of ≤0.5 pixel for orders 2–9 (orders 1 and 10 were not used in this analysis due to low signal). The background sky was taken from the edges of the slit, farthest from the galaxy centre. Although some faint background light from the galaxy may be contained in the sky apertures, there was no indication of the Calcium Triplet (CaT) absorption lines in the sky spectrum, so this appears to be a very small effect.

4 SIZE MEASUREMENTS

Archival Subaru suprime-cam imaging of LEDA 074886 in the g band under 0.7 arcsec seeing conditions reveals an unresolved nucleus. Surrounding this is an elongated, discy structure (see Fig. 2). The outer regions of the galaxy become very boxy. We modelled the galaxy isophotes using the IRAF task ellipse. This fitting process models each isophote with an ellipse that includes higher order Fourier components for boxyness and discyness. However, it is not ideal for galaxies that are extremely discy; therefore, our Sérsic profile fits to the 1D surface brightness profile should be regarded as somewhat tentative. We measure a Sérsic index $n \sim 1$ and a geometric mean $R_e \sim 9$ arcsec. The nucleus contributes <1 per cent to the total galaxy luminosity. We note that these measurements are not used in the subsequent analysis as it appears from our imaging, and our spectral analysis below, that LEDA 074886 is not a pressure-supported dE galaxy (as is classified by Trentham & Tully 2006) but rather a late-type dwarf galaxy. We do, however, present the dynamical information for this galaxy here.

After reducing the ESI images of PGC 032348 using standard methods with the IRAF software, the galaxy isophotes were fitted with the IRAF task ellipse. A point-source plus Sérsic fit to the resulting B (R) band surface brightness profile gave $n = 1.1$ (1.2) and a geometric mean effective radius of $R_e = 11.9$ arcsec (11.4 arcsec). The galaxy reveals an unresolved nucleus with a luminosity contribution of <0.5 per cent to the total galaxy light. An image of PGC 032348 and the B-band surface brightness profile are shown in Figs 3 and 4.

The geometric mean R_e for the three Virgo cluster dEs are taken from Janz & Lisker (2008) who carried out Sérsic fits to the g-band surface brightness profiles from SDSS images.

5 VELOCITY MEASUREMENTS

For PGC 032348 and VCC 846, the S/N of our spectra is such that we were only able to extract a single aperture that corresponds roughly to the full width at half-maximum size of the 2D galaxy spectrum. For the other three galaxies in the sample, we extracted a central aperture of ±3 pixels (0.9 arcsec), which is of the order of the seeing. Additional independent apertures were also extracted on either side of the galaxy centre. The size of the off-centre extraction apertures was designed to achieve a similar S/N independent of the radius. In Fig. 5, we show the central aperture extraction centred around 8500 Å for all five galaxies. This wavelength region includes the CaT lines which are used to obtain velocity and velocity dispersion measurements.

To obtain recession velocity and velocity dispersion measurements, we selected stellar templates from two high-resolution stellar libraries (Montes et al. 1997 in the CaT region, and Bagnulo et al. 2008 in the Mg and Fe line region) covering a range of spectral types. These template stars were first broadened to the same spectral resolution as our data. We used the PPXF code of Cappellari & Emsellem (2004) to measure the first and second velocity moments

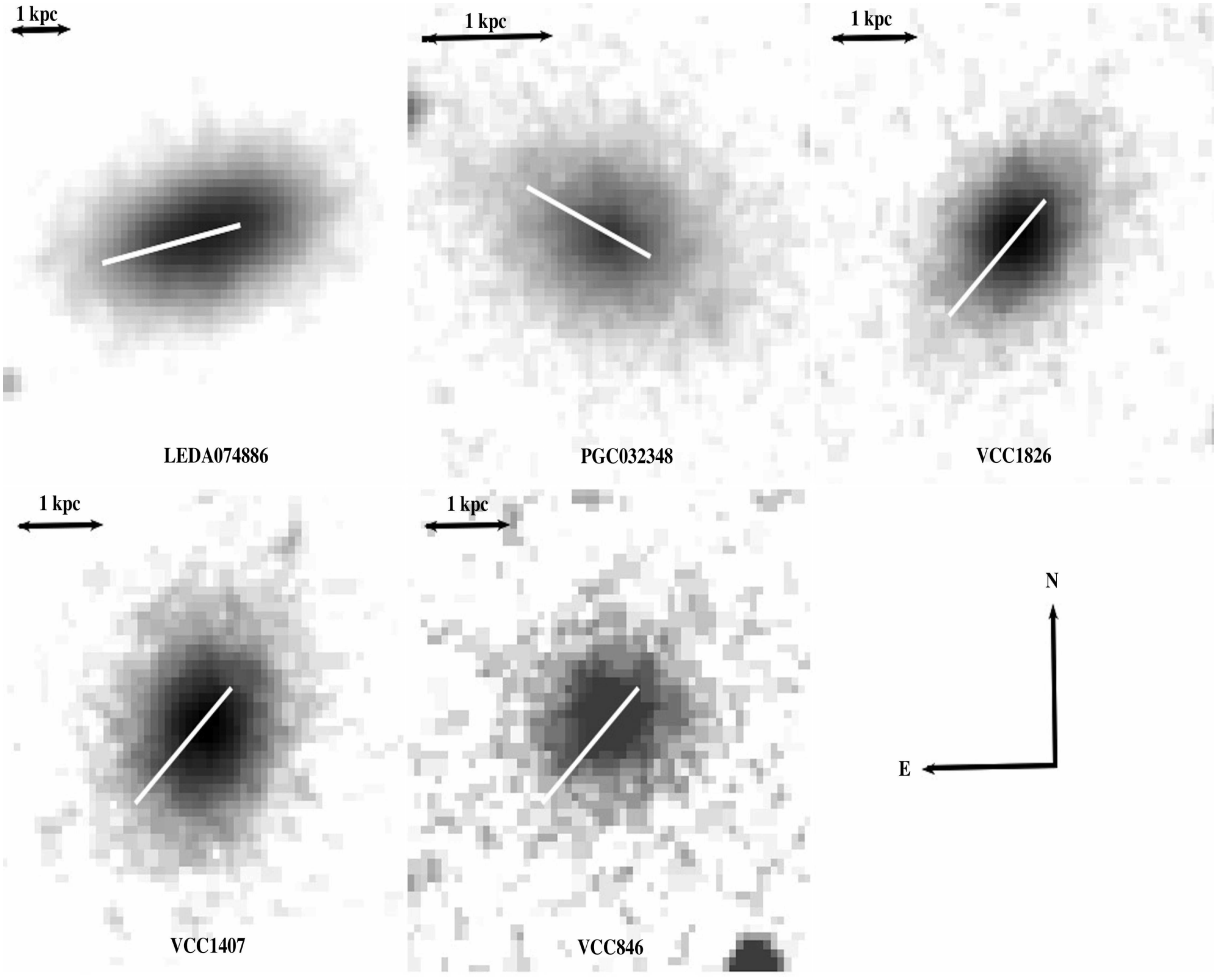

Figure 1. Montage of the dwarf galaxy sample. The orientation and length of the ESI slit is shown on images from the DSS. North is up and east is to the left-hand side. A 1-kpc scale bar is shown in each image.

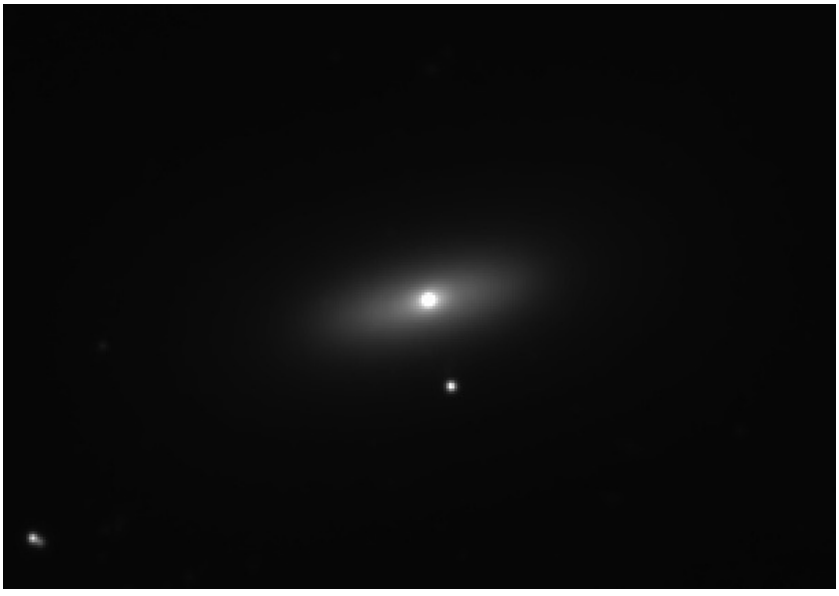

Figure 2. Image of LEDA 074886. The image size is approximately 60×45 arcsec^2. North is up and east is to the left-hand side. At the distance of LEDA 074886, 1 arcsec equals 120 pc. The central nucleus and inner elongated disc structure is clearly seen.

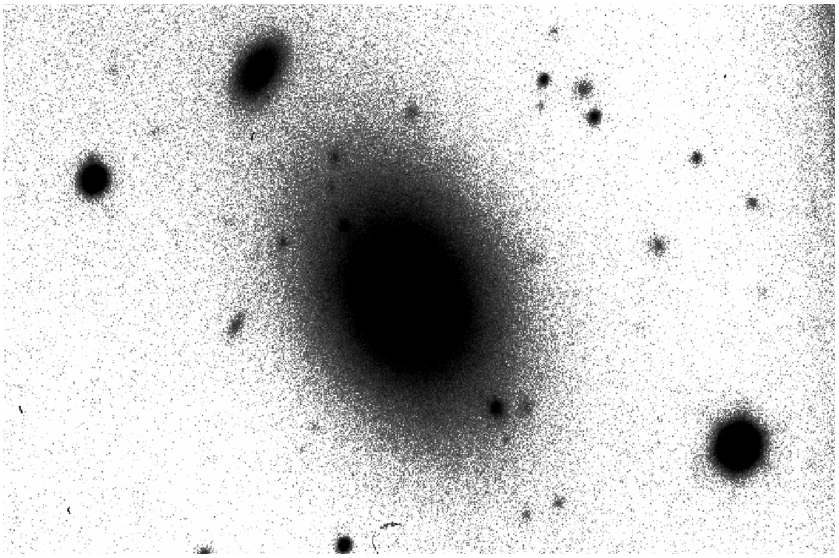

Figure 3. Negative image of PGC 032348. The image size is 105 × 70 arcsec^2 in size. North is up and east is to the left-hand side. At the distance of PGC 032348, 1 arcsec equals 53 pc.

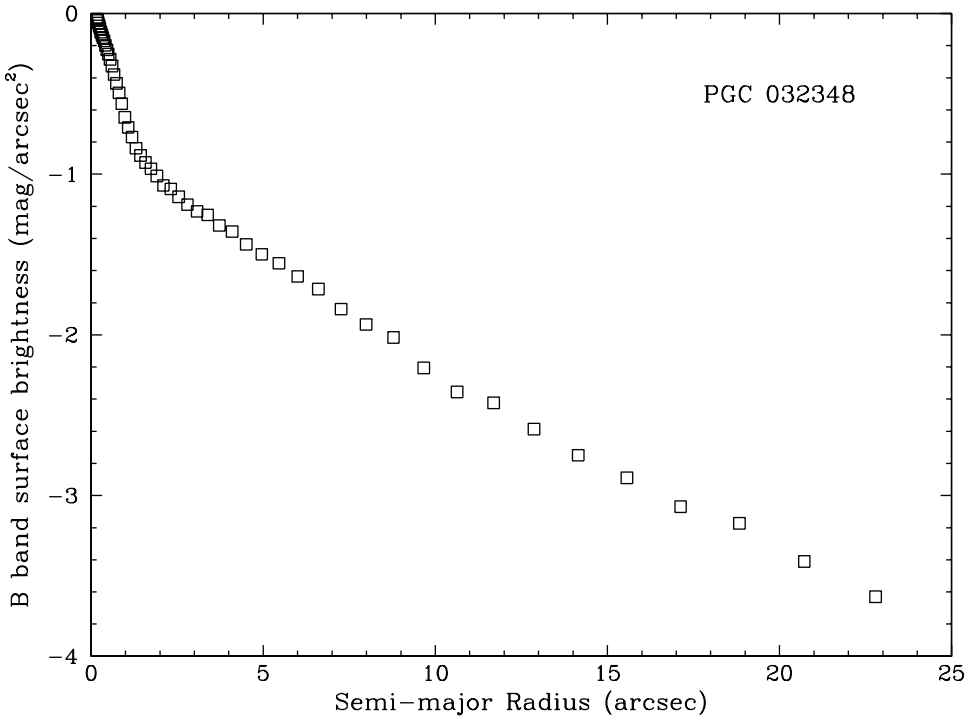

Figure 4. *B*-band surface brightness profile of PGC 032348. The surface brightness has been normalized to the galaxy centre.

of our galaxies (i.e. recession velocity and velocity dispersion). The PPXF routine simultaneously shifts, broadens and determines the best set of weighted template stellar spectra that minimizes the residuals between the science spectrum and the fit. Spectral regions affected by strong skylines are manually excluded from the fit. This approach minimizes errors due to template mismatch by allowing the simultaneous use of multiple possible templates (in our case, typically, a dozen per galaxy). It also allows for the fact that giant stars dominate the near-infrared (i.e. CaT region), whereas dwarf stars may have an increased contribution in the optical (i.e. Mg and Fe line region).

As an independent confirmation of our measurements, we also ran PPXF using a *single* stellar spectrum taken on the same observing run with the same slitwidth as our galaxy spectra. The shifted and broadened stellar spectrum of this star (HR224) provided a good match to the Mg and Fe lines and thus provides another measure of the velocity moments. The resulting velocity profiles are shown in Figs 6–8 with radii at the mid-point of the aperture.

For the three galaxies with off-nuclear apertures, a second-order polynomial fit to the off-nuclear apertures was taken as representative of the galaxy velocity dispersion profile. The interpolated value

© 2011 The Authors, MNRAS **413,** 2665–2678
Monthly Notices of the Royal Astronomical Society © 2011 RAS

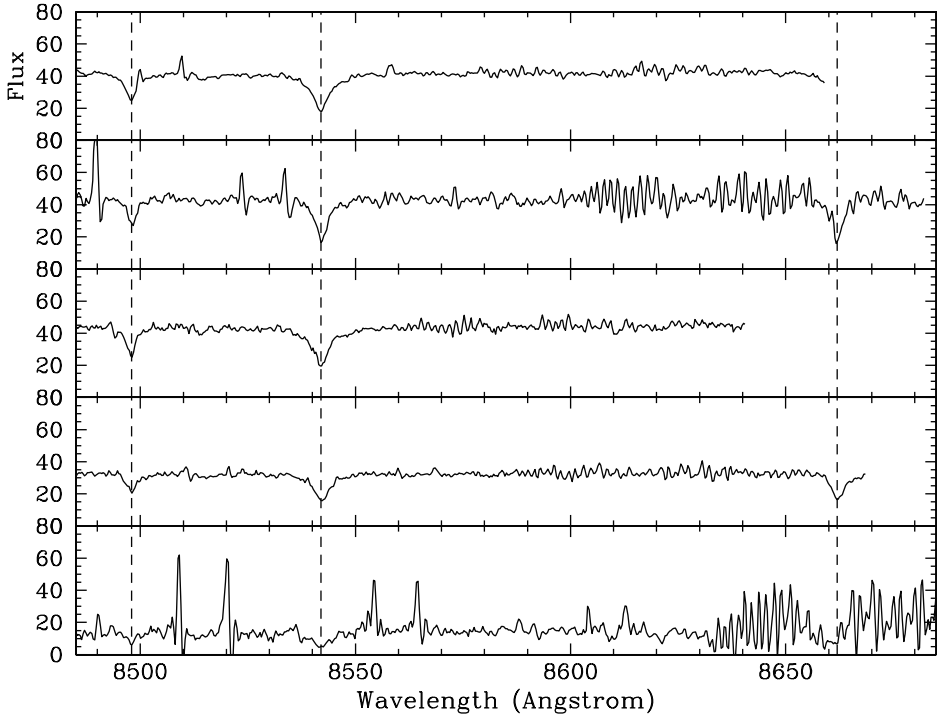

Figure 5. ESI spectra of dwarf galaxies. Top to bottom are LEDA 074886, PGC 03248, VCC 1826, VCC 1407 and VCC 846, respectively. The rest-wavelength spectra show the central aperture extraction for each dwarf galaxy. The three CaT lines (8498, 8542 and 8662 Å) are indicated by the dashed lines. Regions affected by skylines are excluded from the spectral fits. For some spectra, only two of the three CaT lines are available.

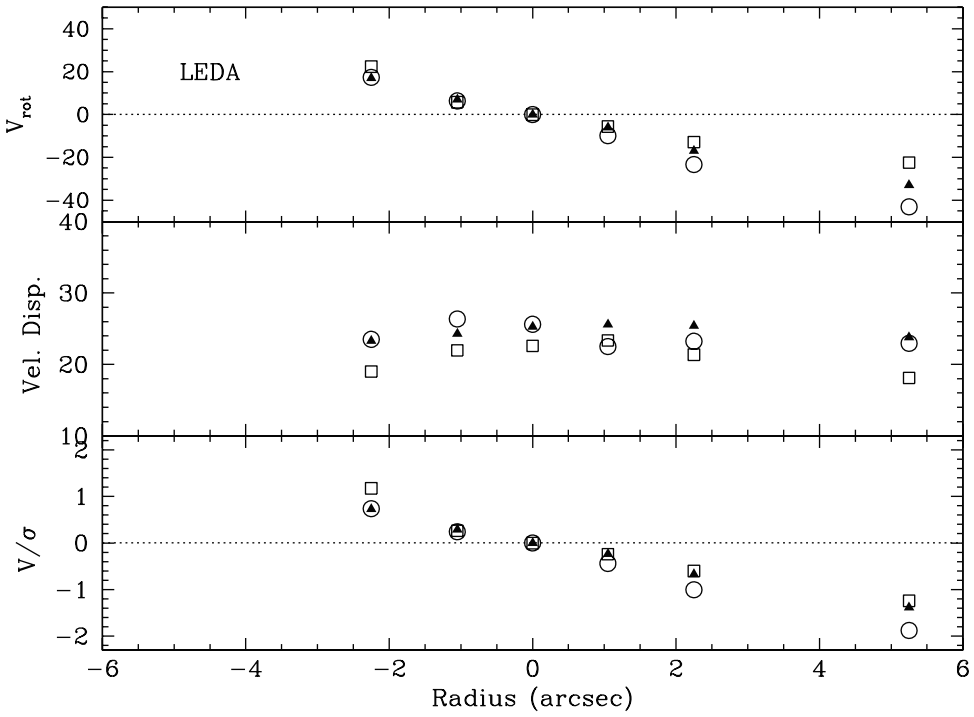

Figure 6. Velocity profile for LEDA 074886. The top panel shows the rotation velocity (normalized to the galaxy systemic velocity at the galaxy centre). The middle panel shows the velocity dispersion. The lower panel shows the V/σ ratio (normalized to zero at the galaxy centre). The symbols show the results from the stellar library fit to the Mg and Fe regions (open squares), the CaT region (open circles) and from the ESI template star to the Mg and Fe regions (filled triangles).

at the galaxy centre is adopted as the galaxy central velocity dispersion, σ_0. The uncertainty in these measurements is assumed to be the full range of velocity dispersions from the Mg and Fe lines compared to those from the CaT lines.

For VCC 846, the velocity dispersion derived from using the stellar library varied from 14 to 24 km s^{-1}, whereas the stellar spectrum of HR224 gave 17 km s^{-1}. We adopt a central velocity dispersion of 19 $\pm$ 5 km s^{-1}. To further confirm this value, we attempted to

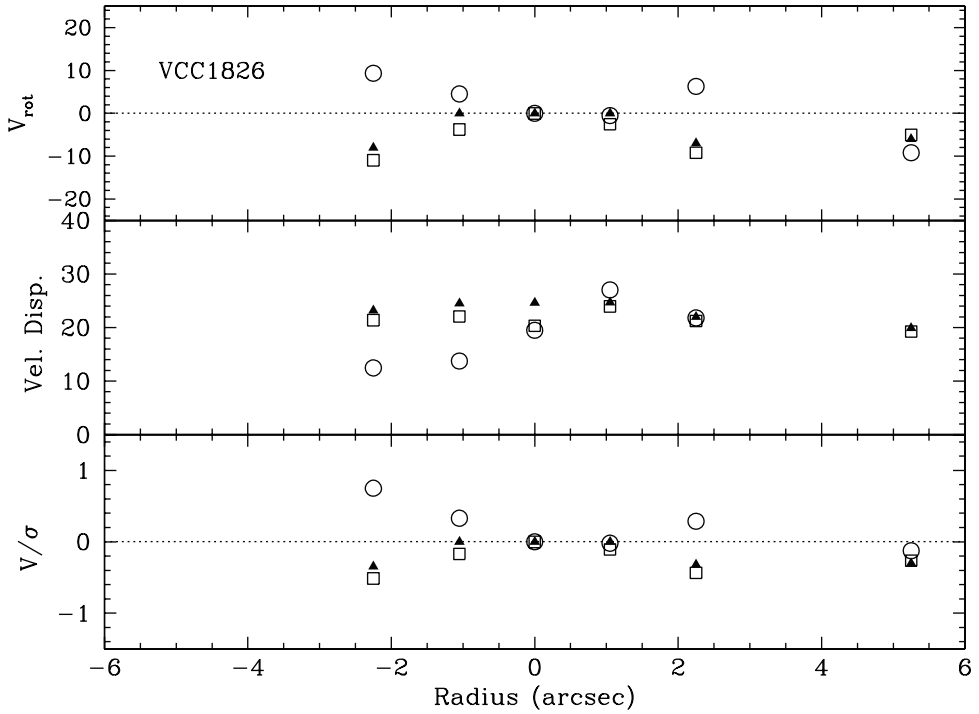

Figure 7. Velocity profile for VCC 1826. The top panel shows the rotation velocity (normalized to the galaxy systemic velocity at the galaxy centre). The middle panel shows the velocity dispersion. The lower panel shows the V/σ ratio (normalized to zero at the galaxy centre). The symbols show the results from the stellar library fit to the Mg and Fe regions (open squares), the CaT region (open circles) and from the ESI template star to the Mg and Fe regions (filled triangles).

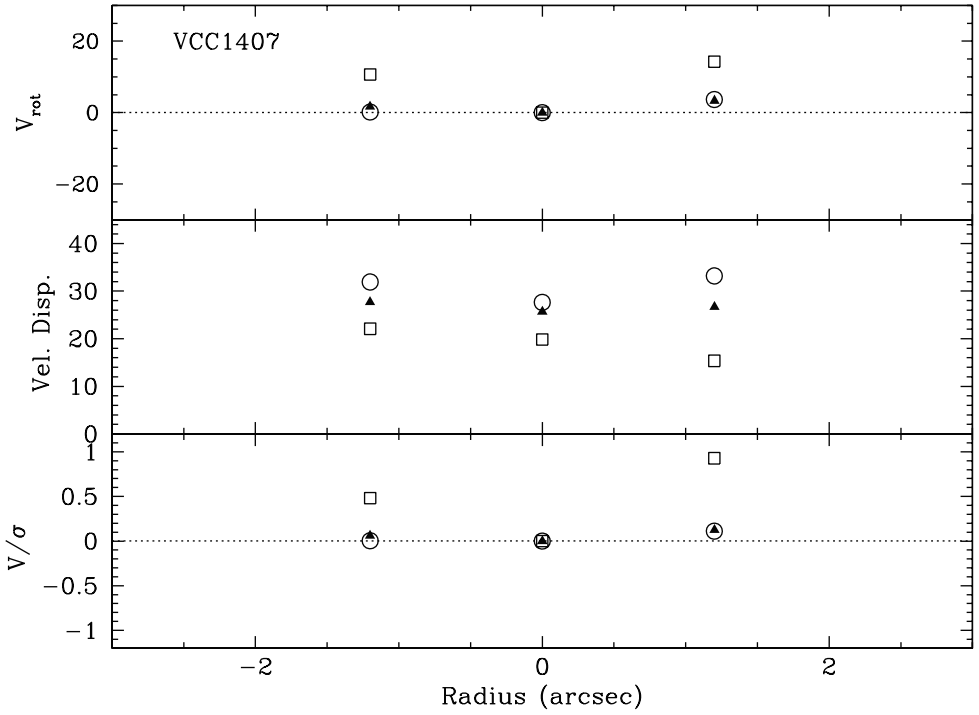

Figure 8. Velocity profile for VCC 1407. The top panel shows the rotation velocity (normalized to the galaxy systemic velocity at the galaxy centre). The middle panel shows the velocity dispersion. The lower panel shows the V/σ ratio (normalized to zero at the galaxy centre). The symbols show the results from the stellar library fit to the Mg and Fe regions (open squares), the CaT region (open circles) and from the ESI template star to the Mg and Fe regions (filled triangles).

measure the velocity dispersion with the Fourier cross-correlation method using the software package FXCOR. This is somewhat more subjective than the PPXF method. We found a preferred value of $20 \pm 10\,\mathrm{km\,s^{-1}}$, that is, consistent with our PPXF value.

For PGC 032348 we derived 13.8 and 17.0 $\mathrm{km\,s^{-1}}$ from the stellar library and 13.9 $\mathrm{km\,s^{-1}}$ using the ESI spectrum of HR224. We adopt a central velocity dispersion of $15.4 \pm 1.6\,\mathrm{km\,s^{-1}}$ for PGC 032348.

Table 3. Velocity dispersion measurements.

Galaxy name	Nucleus σ_N (km s^{-1})	Galaxy σ_0 (km s^{-1})
LEDA 074886	24.1 ± 1.5	22.9 ± 0.6
PGC 032348	–	15.4 ± 1.6
VCC 1826	19.9 ± 0.5	22.3 ± 2.2
VCC 1407	23.7 ± 3.9	25.5 ± 1.5
VCC 846	–	19 ± 5

Notes. σ_N is the velocity dispersion measured at the nucleus and σ_0 is the velocity dispersion interpolated at the galaxy centre.

Finally, we note that VCC 1407 was observed using the ESI with a 0.75-arcsec slit by Evstigneeva et al. (2007). They extracted a single 1.5-arcsec aperture about the galaxy centre. From measurements of the Mg, Fe and CaT regions, they adopted a velocity dispersion of 30.4 ± 2.6 km s^{-1} over their aperture. A central velocity dispersion of 36 ± 5 km s^{-1} was derived from a medium-resolution ($R \sim 5000$) poor S/N spectrum by Chilingarian (2009). Our adopted central galaxy velocity is $\sigma_0 = 25.5 \pm 1.5$ km s^{-1}.

The adopted central galaxy (σ_0) and nuclear aperture (σ_N) velocity dispersions for each galaxy are given in Table 3.

6 VELOCITY PROFILES

We have measured velocity profiles for three of our sample dE galaxies beyond the nucleus (see Figs 6–8). Two of the galaxies are dominated by random motions with no evidence for ordered rotation (although even at the largest radius probed, our data are still within the effective radius). For the LEDA 074886 galaxy, we find strong evidence of rotation, with a velocity of $\sim$30 km s^{-1} and $V/\sigma \geq 1$ (indicative of a disc) at the largest radii probed ($\sim 0.5 R_e$). Thus, LEDA 074886 is not pressure-supported in its inner regions (we continue to list LEDA 074886 in the tables but it is not shown in subsequent figures). Our data are confined to the inner disc structure seen in the Subaru imaging (see Fig. 2). The velocity dispersion profiles of all the galaxies show little or no trend with the radius. Our interpolated galaxy central σ_0 values are all consistent with the nuclear value σ_N, indicating that the nucleus does not strongly affect the central kinematics in our sample galaxies (i.e. we see no evidence for central dips or peaks in the velocity dispersion).

7 INDIVIDUAL GALAXY NOTES

7.1 LEDA 074886

Classified as a non-nucleated dE, LEDA 074886 is a confirmed member of the NGC 1407 group with a recession velocity $V = 1394$ km s^{-1} (Brough et al. 2006). With $M_K = -19.79$ mag, it is the highest-luminosity galaxy in our sample. It may be interacting with the giant elliptical NGC 1407 ($V = 1779$ km s^{-1}) as it lies at a projected distance of only 8.4 arcmin or 61 kpc from its centre.

Subaru suprime-cam imaging in 0.7-arcsec seeing indicates an elongated, discy structure in the galaxy central regions (see Fig. 2). A small unresolved nucleus is seen at the galaxy centre. The galaxy bears a resemblance to the post-tidal stripping model galaxy shown in fig. 1 of Mayer et al. (2007).

Both the imaging and our velocity profiles suggest that the galaxy contains a thin embedded inner disc with ordered rotation. It is not a pressure-supported system in its inner regions and we exclude it from subsequent figures.

7.2 PGC 032348

This Leo group galaxy is listed as the dE,N galaxy CGCG 066−026 by Trentham & Tully (2002), who quoted an R magnitude of 14.64. Our ESI imaging (see Fig. 3) reveals an unresolved nucleus with a luminosity contribution of <0.5 per cent.

7.3 VCC 1826

This Virgo dwarf galaxy was imaged as part of the ACS Virgo Cluster Survey. Sérsic fits to ACS images by Côté et al. (2006) give nuclear parameters of $g = 20.12$ and $z = 18.91$ for a small unresolved nucleus. The nucleus represents <2 per cent of the total galaxy flux. There is no nearby large galaxy.

7.4 VCC 1407

This Virgo dwarf galaxy was imaged as part of the ACS Virgo Cluster Survey. Sérsic fits to ACS images by Côté et al. (2006) give nuclear parameters of $g = 20.40$ and $z = 19.40$ for a nucleus of a half-light size = 0.127 arcsec (11.6 pc). The nucleus represents <2 per cent of the total galaxy flux. There is no nearby large galaxy.

7.5 VCC 846

VCC 846 is projected close to M87 but has a large blueshifted velocity of -730 km s^{-1} [NASA Extragalactic Data base (NED)]. However, the surface brightness fluctuation study of Jerjen, Binggeli & Barazza (2004) confirms its Virgo cluster membership. Barazza, Binggeli & Jerjen (2003) list a B-band $R_e = 12.35$ arcsec and a Sérsic index n value = 0.6. The Virgo spiral galaxy NGC 4402 lies at a projected distance of 31 kpc.

8 ADDITIONAL DATA SAMPLES

To supplement our data on low-mass dE galaxies, we include literature data for other dwarf systems of similar mass. These include higher mass dEs and lower mass dSph galaxies and UCD objects (which may be galaxies or simply massive star clusters). All of these systems are pressure-supported in their inner regions, dominated by stars of old age, reveal smooth featureless morphologies and contain little or no gas (so that stellar masses are a good proxy for baryonic masses).

We note that the kinematic study of 73 galaxies by Simien & Prugniel (2002) includes some dwarf galaxies. The lowest luminosity with $M_B = -13.5$ mag ($M_K \sim -15.5$ mag) and $\sigma_0 = 25 \pm 16$ km s^{-1} is UGC 5442; however, it is classified as a late-type Im galaxy. The lowest-luminosity elliptical galaxy is PGC 39385 with $M_B = -14.48$ mag (and $M_K = -18.07$ mag from the 2MASS) and $\sigma_0 = 19 \pm 6$ km s^{-1}. Simien & Prugniel (2002) quote an effective radius for UGC 5442 but not for PGC 39385. We have not used any data from the Simien & Prugniel (2002) study in this work.

8.1 Virgo cluster dE galaxies

The internal dynamics of 17 dE galaxies in the Virgo cluster were studied by Geha et al. (2002,2003) using the ESI on Keck. The main difference from our work is that they focused on brighter, more-luminous dEs and they used a 0.75-arcsec slit (which has an effective resolution of 23.7 versus our 15.8 km s^{-1}). Their sample is also dominated by galaxies with nuclei, that is, classified as dE,N.

They derive the average velocity dispersion for radii beyond 1 arcsec to avoid nuclear contamination. Their velocity dispersion profiles reveal central dips and peaks, but are otherwise generally flat beyond 1 arcsec. We take their value as a reasonable measure of the galaxy central velocity dispersion. As with our three Virgo dEs, we take the R_e sizes from Janz & Lisker (2008).

K-band photometry exists for 14/17 galaxies from the 2MASS. For the remaining three galaxies, we take the g-band magnitude from Janz & Lisker (2009) and apply a $g - K = 2.5$ transformation (equivalent to [Fe/H] $= -1.3$).

These data are supplemented by additional Virgo dE measurements from Chilingarian (2009). Here the off-nucleus velocity dispersions come from a variety of medium-resolution (resolution $\sim 50\,\mathrm{km\,s^{-1}}$) spectra taken using different telescopes and instruments. Metallicities are also derived from the spectra. We use K-band magnitudes from the 2MASS and R_e sizes from Janz & Lisker (2008). We find that the Chilingarian data have a larger scatter for a given galaxy mass than the Geha et al. data. This is likely due to the poorer spectral resolution of the Chilingarian data.

As above, we assume a distance modulus to the Virgo cluster of $m - M = 31.09$.

8.2 Local Group dSph galaxies

For the Milky Way satellite dSph galaxies, we use the compilation of Wolf et al. (2010). From this we use their R_e size (in parsecs), velocity dispersions and V-band luminosities. We note that the R_e sizes may not be directly comparable to those for dEs as they are often major-axis values from exponential fits to surface brightness profiles rather than geometric mean values from Sérsic law fits. In addition, velocity dispersions for dSph galaxies are generally measured from individual stars rather than integrated light. Metallicities for the individual dSph galaxies come from Kirby et al. (2009). For M31 dSph galaxies, we use the recent studies of Kalirai et al. (2010) and Collins et al. (2010) to obtain velocity dispersions, V-band luminosities, R_e sizes (in parsecs) and metallicities.

8.3 Local Group dE galaxies

We take R_e sizes and the average galaxy velocity dispersions for the three Local Group peculiar dE galaxies (NGC 147, 185, and 205) from De Rijcke et al. (2006). Distance moduli and metallicities are assumed to be $m - M = 24.43$, 24.23 and 24.57 and [Fe/H] $= -1.0$, -1.2 and -0.9 for NGC 147, 185 and 205, respectively. We use K-band magnitudes from the 2MASS Large Galaxy Atlas. We note that extinction-corrected V-band magnitudes from the RC3 would result in slightly lower stellar masses.

8.4 Ultracompact dwarfs

Here we adopt the working definition of an UCD as a compact ($R_e \leq 100\,\mathrm{pc}$) near-spherical object of mass greater than $2 \times 10^6$7thinsp;$\mathrm{M}_\odot$. This mass limit represents a (somewhat arbitrary) separation from lower-mass GCs and corresponds to a relaxation time-scale that is longer than the Hubble time (Dabringhausen et al. 2008). It also corresponds to the mass above which UCDs reveal a mass–metallicity and a size–mass relation that is not present in lower-mass GCs (Forbes et al. 2008). Data for UCDs come from the homogeneous data base of Mieske et al. (2008), which includes mostly Virgo and Fornax cluster objects. From this we take their R_e sizes, metallicities and their aperture-corrected velocity dispersions. Total K-band magnitudes come from the 2MASS where possible; otherwise, the V-band magnitude from the original source as listed by Mieske et al. (2008) is used. We have excluded the two very large, luminous objects (F-19 and VUCD7) for which the velocity dispersion is taken from the core, while the effective radius and luminosity relate to the core plus halo (see also Evstigneeva et al. 2008).

Table 4. Derived properties.

Galaxy name	$M_{\rm dyn}$ ($\times 10^8\,\mathrm{M}_\odot$)	M_* ($\times 10^8\,\mathrm{M}_\odot$)
LEDA 074886	5.5	19.7
PGC 032348	1.5	0.87
VCC 1826	2.5	1.5
VCC 1407	4.7	3.8
VCC 846	3.4	1.7

Notes. $M_{\rm dyn}$ is the dynamical mass within the 3D half-light radius and M_* is the *total* stellar mass (see text for details).

9 MASS ESTIMATES

9.1 Stellar masses

Stellar masses are derived from K-band magnitudes where possible and V band otherwise. The resulting luminosities are multiplied by a stellar mass-to-light ratio (M/L), in the appropriate band, from a single stellar population model (Bruzual & Charlot 2003). The M/L varies with the galaxy metallicity (or colour) for an assumed fixed mean age of 12 Gyr and a Chabrier initial mass function (IMF). The advantage of working in the K band is that it is a good proxy for the stellar mass with the M/L being less sensitive to metallicity variations than optical bands. If the mean age of the stars were 5 Gyr, then the M/L would be systematically lower by a factor of about 2, although for the systems studied here the stellar mass is dominated by old-age stars. Variations due to different simple stellar population models and IMFs have been explored by Dabringhausen et al. (2008). Thus, from the total luminosity, we derive the total stellar mass, listed in Table 4. To calculate the stellar mass within the effective radius, we simply divide the *total* stellar mass by 2. As these systems are largely devoid of gas, the stellar mass is equivalent to the baryonic mass.

9.2 Dynamical masses

Dynamical mass estimates of non-rotating, pressure-supported systems are typically obtained using the expression

$$M_{\rm dyn} = C\sigma^2 R, \quad (1)$$

where R is a measure of the size of the system and σ a measure of the system's velocity dispersion (Djorgovski, de Carvalho & Han 1988). The size of a system is often taken to be the effective, or half-light, radius (R_e) which can be measured from a surface brightness profile. The observed σ, however, is often simply a central value. In principle, this can be corrected to a uniform standard (such as the total, luminosity-weighted, infinite-aperture, velocity dispersion) via the variable term C. This coefficient can allow for dynamical non-homology (e.g. a range of different velocity dispersion profile shapes).

The difference between some central aperture velocity dispersion measurement and the total aperture velocity dispersion is greater for the more highly concentrated systems which have high Sérsic

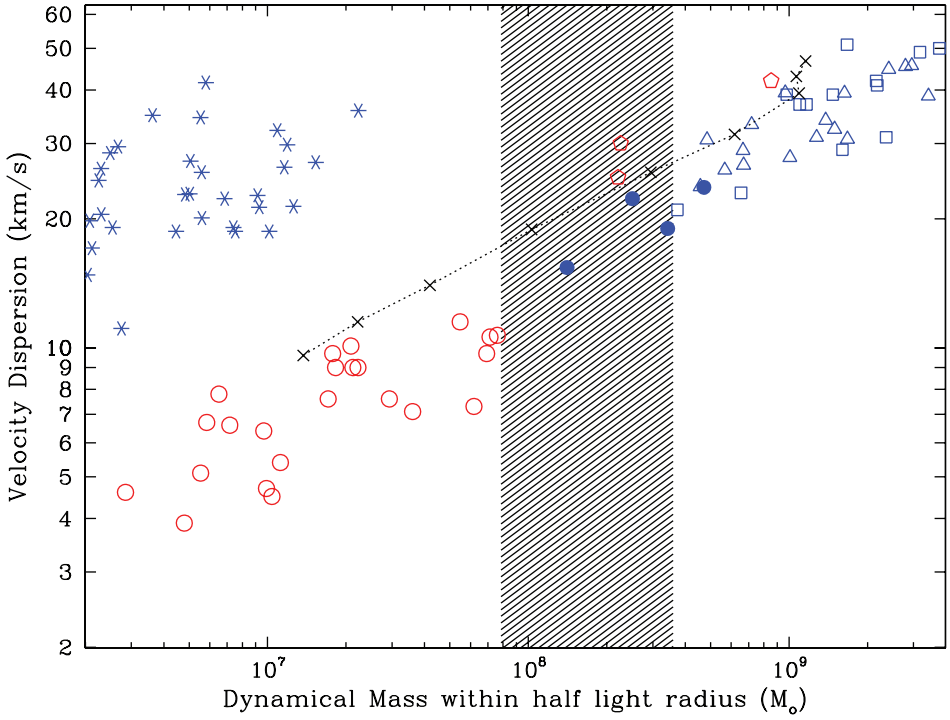

Figure 9. Dwarf galaxy velocity dispersion versus dynamical mass within the deprojected half-light radius (equal to $4/3R_e$). Symbols are as follows: red for dwarfs located in the Local Group and blue for external dwarfs, with the open circles for Milky Way and M31 dSph galaxies (Wolf et al. 2010), open pentagons for Local Group dE galaxies (NGC 147, 185 and 205; De Rijcke et al. 2006), stars for UCDs (Mieske et al. 2008), and open triangles (Chilingarian 2009) and squares (Geha et al. 2003) for Virgo dE galaxies. Our new data are shown by the filled blue circles. The dynamical mass is calculated using the technique of Wolf et al. (2010) which has the advantage of being robust to the actual 3D orbits of the dynamical tracer stars. The shaded region shows the dynamical mass gap between external dE galaxies and dSph galaxies. The dotted lines and crosses show the *N*-body/smoothed particle hydrodynamic (SPH) models of dwarf galaxies from Valcke et al. (2008). Our new data suggest a continuous trend in the velocity dispersion from dE galaxies to the lower-mass dSph galaxies, rather than the UCDs.

indices and, through the Jeans equation (Ciotti 1991), also possess steeper aperture velocity dispersion profiles (Ciotti, Lanzoni & Renzini 1996; Busarello et al. 1997; Graham & Colless 1997; Prugniel & Simien 1997; Simonneau & Prada 2004). Bertin, Ciotti & Del Principe (2002) have calculated the value of C to be used with central velocity dispersions (within $1/8R_e$) as a function of the Sérsic index n, showing that C roughly equals 8, 4 and <2 when n equals 1, 4 and >10, respectively. While this variable term is needed, the long-recognized problem is that these corrections are based on models having orbital isotropy (Ciotti & Lanzoni 1997; Mamon & Boué 2010). Large contributions from radial or tangential orbits will skew these mass estimates.

Recently, Wolf et al. (2010, their equation 1) report that, independent of orbital anisotropy, the mass enclosed within a spherical volume of radius r_3 can be approximated by $3r_3\ \langle\sigma^2_{\rm total}\rangle/G$ when $\langle\sigma_{\rm total}\rangle$ is the luminosity-weighted, infinite-aperture velocity dispersion and r_3 is the radius where the internal 3D density profile has a slope equal to -3. Given (i) the observation from Graham et al. (2006, their fig. 9) that the slope of density profiles is close to a value of -3 at their deprojected half-light radii coupled with (ii) Ciotti's (1991) finding that the deprojected half-light radius is very close to 4/3 times the projected half-light radius R_e, the mass can be approximated as $4R_e\ \langle\sigma^2_{\rm total}\rangle/G$ (see also equation 2 and appendix B of Wolf et al.).

In this work, we do not have total aperture velocity dispersions, but rather central aperture velocity dispersions (σ_0). However, we note that the aperture velocity dispersion profiles of systems with Sérsic indices approximately less than 2 are expected to be flat (e.g. Graham & Colless 1997; Simonneau & Prada 2004). Indeed, the velocity dispersion profile of the Local Group dEs NGC 147 and 185 (Geha et al. 2010) is observed to be flat out to $1R_e$, and even to $5R_e$, using resolved star measurements. The UCDs, dSph and dEs examined here typically have Sérsic indices of $0.5 < n < 2$. We therefore use our central velocity dispersions as a proxy for the total, luminosity-weighted, aperture velocity dispersions.

In Table 4, we list the dynamical mass calculated using equation (1) with R_e as the size, σ_0 as the velocity dispersion and a coefficient of $C = 4$. This corresponds to the mass within a sphere containing half the system's light, rather than the entire system's mass. Dividing this mass by half of the galaxy's total light gives the M/L within the deprojected half-light radius.

In passing, we again note that a word of caution is warranted. We are able to use equation (1), with a constant C term, to approximate the mass, because we are dealing with dwarf systems which have flat velocity dispersion profiles. The velocity dispersion profiles of luminous elliptical galaxies, however, are not the same, instead being centrally peaked. Consequently, the luminosity-weighted, infinite-aperture velocity dispersion for these galaxies can be significantly different from the available (typically central) value. It is the former quantity which is required in equation (1) and obviously the use of a single coefficient in this equation cannot correct the central velocity dispersion for all of these varying differences. For this reason, Wolf et al. (2010) note that this equation approximates the mass 'under the assumption that the observed (luminosity-weighted) stellar velocity dispersion profile is relatively flat near (and beyond) R_e' and that one actually uses the luminosity-weighted velocity dispersion

within R_e in this equation. Any mass or Fundamental Plane analysis including luminous elliptical galaxies will introduce a systematic bias with mass if central velocity dispersions are used together with a constant coefficient in equation (1). One method of compensating for this is to adopt a variable coefficient, as tabulated by Bertin et al. (2002).

10 RESULTS AND DISCUSSION

In Fig. 9, we show our new velocity dispersion measurements versus the derived dynamical mass within the half-light radius for our four dE galaxies plus other pressure-supported dwarf systems. We also highlight the mass gap ($8 \times 10^7 < M_{\rm dyn}/{\rm M}_\odot < 5 \times 10^8$) defined to lie between the lowest-mass dEs beyond the Local Group and the highest-mass dSph galaxies. As well as two peculiar Local Group dE galaxies (NGC 147 and 185), the gap now includes three more dE galaxies (the Leo group galaxy PGC 032348, and the Virgo cluster galaxies VCC 1826 and VCC 846). The two peculiar dEs from the Local Group hint at a connection with UCDs; however, the addition of the three new dEs strongly indicates a continuous trend of a declining velocity dispersion with declining dynamical mass, from dEs to the lower-mass dSph galaxies. The slope of the relation ($M_{\rm dyn} \sim \sigma^{2-3}$) is similar to that found by others for dE and dSph galaxies when the luminosity (stellar mass) is considered (e.g. De Rijcke et al. 2005).

Fig. 10 shows the effective radius in parsecs as a function of the dynamical mass within the half-light radius. The galaxies in the mass gap have effective radii that are comparable to that of the most-massive dSph galaxies. Thus, a continuity exists, albeit with a change in the slope (Graham et al. 2006; Graham & Worley 2008; Misgeld, Hilker & Mieske 2009), between the effective sizes of dSph and dE galaxies over a range of greater than 1000 in mass. We note that such continuous trends are now recognized to extend all the way from dEs to giant ellipticals (Graham & Guzmán 2003; Côté et al. 2006; Misgeld et al. 2009).

The UCDs have sizes that are on average about one-tenth those of dSph galaxies. We note that the size–mass trend for UCDs is consistent with models by Murray (2009) that describe optically thick star clusters without DM. This provides further support for the claims that UCDs are simply massive star clusters.

The continuous trends of decreasing velocity dispersion and effective radius with decreasing mass from dEs to dSph galaxies (Figs 9 and 10) are qualitatively similar to the model predictions for an early cosmological origin for dwarf galaxies of Nagashima et al. (2005) and Valcke et al. (2008). In Figs 9 and 10, we overplot the 'C' models from table 3 of Valcke et al. which represent the final (after 10 Gyr) properties of their model galaxies. We calculate the dynamical mass of their model galaxies using equation (1). The models have a similar trend to the data, but are offset in both the velocity dispersion and effective radius. A key ingredient in dwarf galaxy formation models is the degree of energy feedback from supernovae which determines the depth of the potential well (Mashchenko et al. 2008). Strong feedback will result in a more diffuse DM halo which has a smaller central velocity dispersion and more extended stellar profile. As noted by Valcke et al. (2008) *'The combination of R_e and central σ [velocity dispersion] thus provide an excellent tool to evaluate the soundness of halo properties within a certain framework of galaxy formation'.*

As most pressure-supported dwarf systems are devoid of gas, the dynamical mass we derive is essentially equal to the mass in stars plus DM. In Fig. 11, we show the ratio of the dynamical mass to the stellar mass within the half-light radius. This ratio is equivalent to a M/L once the effects of stellar metallicity have been removed. A ratio of unity indicates that the dynamical mass equals

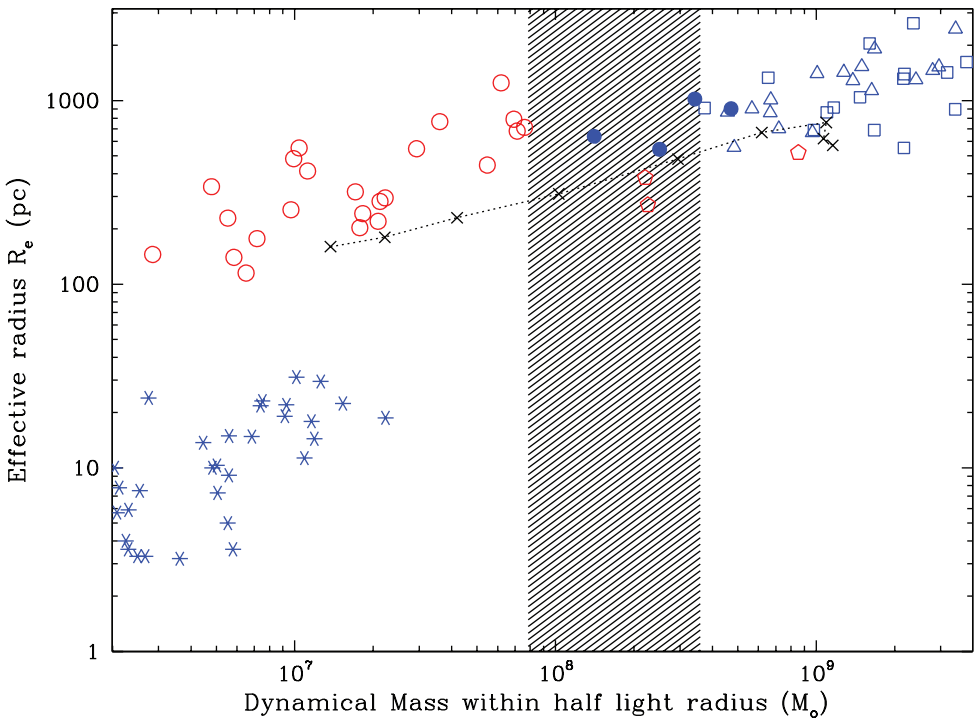

Figure 10. Dwarf galaxy effective radius (R_e) versus dynamical mass. The same symbols as Fig. 9. The dotted lines and crosses show the *N*-body/SPH models of dwarf galaxies from Valcke et al. (2008). Although a slight change in the slope is apparent, the new data again indicate a continuous trend from dE to lower-mass dSph galaxies.

© 2011 The Authors, MNRAS **413,** 2665–2678
Monthly Notices of the Royal Astronomical Society © 2011 RAS

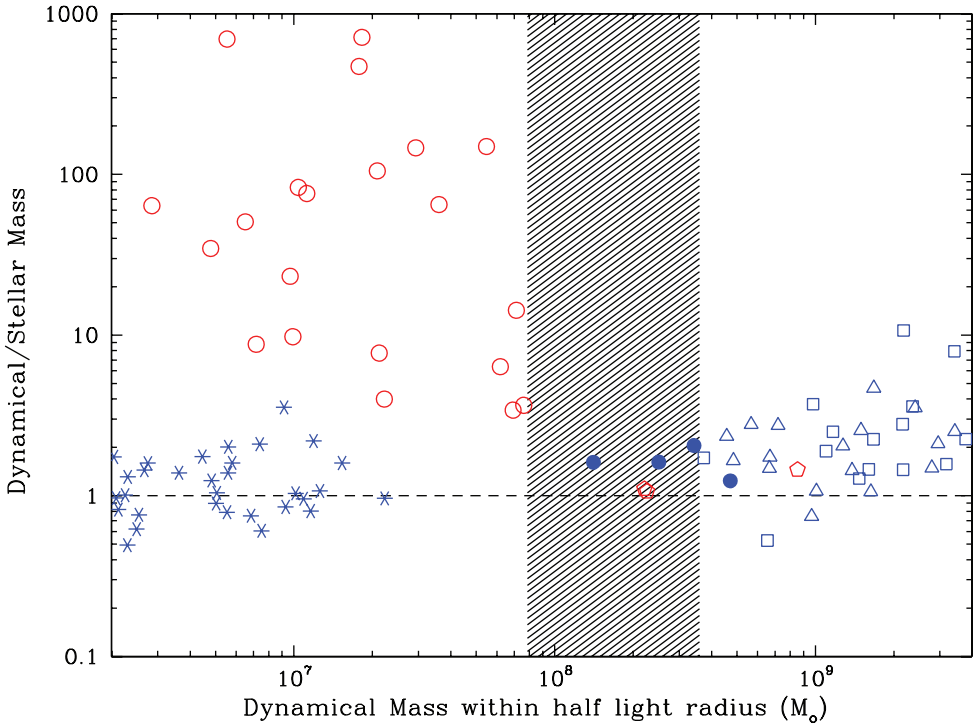

Figure 11. The dynamical-to-stellar mass ratio versus dynamical mass within the deprojected half light radius for dwarf galaxies. The same symbols as Fig. 9. The stellar mass is calculated from an observed total luminosity times a M/L (in the appropriate photometric band) that depends on the metallicity from stellar population models (Bruzual & Charlot 2003). We assume a fixed age of 12 Gyr as dwarfs tend to be dominated by old-age stars. The total stellar mass is then divided by 2 to give the stellar mass within the half-light radius. A ratio of unity, shown by the dashed line, indicates when the dynamical mass equals the stellar mass. The UCD objects scatter about a value of unity, consistent with them being DM-free star clusters. Both the Local Group dE galaxies (NGC 147 and 185) and the new data indicate that there is little, or no, evidence for DM in mass 'gap' galaxies in their inner regions. The dSph galaxies show a rapidly rising ratio (indicative of more DM) for dynamical masses less than 8×10^7 $M_\odot$. There is also a hint of an upturn for the most-massive dE galaxies, suggesting that DM may start to play a role within their inner regions. The gap galaxies are star-dominated like dE galaxies and do not reveal an 'upturn' in their dynamical-to-stellar mass ratio as seen for the apparently DM-dominated dSph galaxies.

the stellar mass within the effective radius, so no DM is required. The UCDs reveal a slightly elevated ratio. This may indicate the presence of some DM or be simply due to a non-standard IMF that is not accounted for in current stellar population models (for more discussion see Dabringhausen et al. 2008; Forbes etal. 2008; Mieske et al. 2008). We note that a change to a more top-heavy IMF with increasing total mass is expected in the optically-thick star cluster model of Murray (2009). The gap galaxies reveal little, or no, evidence for DM in their inner regions. This is in stark contrast to the dSph galaxies which show a rapidly rising ratio (indicative of more DM) for dynamical masses less than 8×10^7 $M_\odot$. Thus, the gap galaxies are star-dominated like higher-mass dE galaxies and do not reveal an increase in their dynamical-to-stellar mass ratio as seen for the DM-dominated dSph galaxies. The gap galaxies may represent a local minimum in the inner region DM fraction for dwarf galaxies in which the process of the gravitational heating of the DM from stellar feedback is at its most-efficient state.

This paper, like Forbes et al. (2008), Dabringhausen et al. (2008) and Mieske et al. (2008), has used three basic quantities: velocity dispersion, size and luminosity. Through the luminosity expression $L = 2\Pi\langle I\rangle_e R_e^2$, involving the mean intensity $\langle I\rangle_e$ inside the half-light radius R_e, our work is in essence a variation of Fundamental Plane studies (Djorgovski & Davis 1987). Throughout the 1990s it was generally thought that galaxies with velocity dispersions less than $\sim$100 km s^{-1}, and thus our dwarf galaxies, were not connected with bright elliptical galaxies because they did not follow the same 2D plane in 3D spaces that used these quantities. Moreover, Bender, Burstein & Faber (1992) had shown that dEs and Es resided in disconnected regions of this 3D parameter space. However, it is now understood that this apparent disconnection was a result of sample selection which missed the bridging population, and Graham & Guzmán (2004) and Graham (2005) have since advocated that the two populations are actually united through a continuous curved distribution of points, noting that the 'Fundamental Plane is simply the tangent sheet to the high luminosity end of a curved surface'. A variant of this manifold was parametrized by Zaritsky, Gonzalez & Zabludoff (2006) and Zaritsky, Zabludoff & Gonzalez (2008), who referred to it as the 'Fundamental Manifold', to which they added disc galaxies, galaxy clusters and dSph galaxies, and GCs (Zaritsky, Zabludoff & Gonzalez 2011). The potentially unifying and curved nature of this surface is receiving renewed interest, although collectively we still need to be careful to account for systematic, mass-dependent variations in galaxy structure and dynamics. The use of a constant C term and central velocity dispersions when dealing with giant elliptical galaxies will misshape the true surface and thus one's conclusions about how the M/L varies across the surface.

In Fig. 12, we show the 3D manifold of the effective radius, dynamical mass and stellar mass for dwarf systems. This can be compared to the recent 3D manifold of the radius, dynamical mass and luminosity presented by Tollerud et al. (2011). Like Tollerud et al., we conclude that UCDs do not follow the general trend seen for dEs and dSph galaxies. Tollerud et al. also discuss the manifold of Zaritsky et al. (2011) that includes GCs and UCDs,

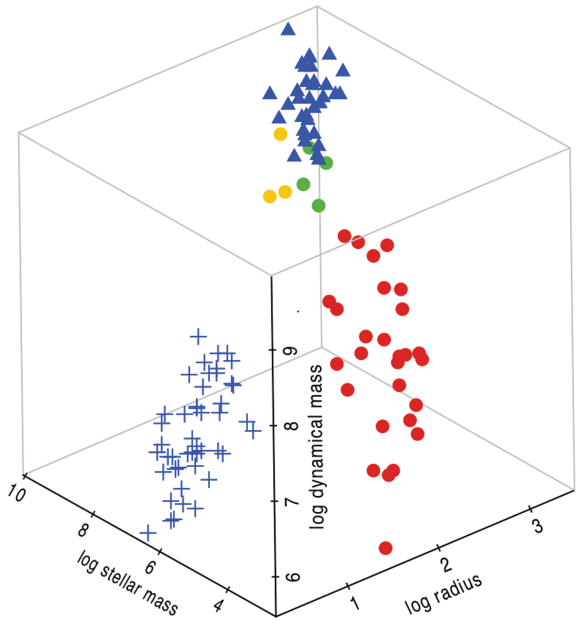

Figure 12. 3D manifold for dwarf systems. The axes are effective radius (in pc), dynamical mass (in solar masses) and stellar mass (in solar masses). Our new data are shown by the green dots, Local Group dEs by the yellow dots, Virgo dEs by the blue triangles, UCDs by the blue crosses and Local Group dSph galaxies by the red circles. Our new data for low-mass dE galaxies reveal a continuous trend from higher mass dEs to dSph galaxies.

as well as dSph and elliptical galaxies. Tollerud et al. present a 3D figure that includes the 'warped' manifold of Zaritsky et al. showing how this can incorporate GCs and UCDs. However, GCs and UCDs occupy a different part of the manifold to dSph galaxies without any bridging population with intermediate properties. In other words, a bifurcation exists at these mass-scales, with UCDs and dSph galaxies occupying different branches. This is consistent with our findings of a different evolutionary history.

Although dE and dSph galaxies form continuous trends in Figs 9 and 10, the dynamical-to-stellar mass ratio trend seen in Fig. 11 suggests a dramatic change in the slope (and DM content) for masses lower than the mass gap. This can be understood in the context of their local environment. All of the dSph galaxies examined here are located within, or near, the halo of a giant galaxy, namely the Milky Way or Andromeda, whereas the dE galaxies are located in groups or clusters and not necessarily within the halo of a massive galaxy. Thus, the evolutionary history of the Local Group dSph galaxies may have been different from that of dwarfs of similar mass that are not subject to the same degree of star and gas removal. The extent of this mass-loss due to stripping depends on the mass, and mass density, of the progenitor galaxy, as well as the strength of the tidal interaction, and the efficiency of forming stars from any gas before it is stripped away (Mayer et al. 2001). These parameters may in turn depend on the epoch of formation of the dwarf galaxy and when it is accreted into a larger halo (Macciò, Kang & Moore 2009). Thus, depending on the exact processes and time-scales, a range of dynamical-to-stellar mass ratios for dwarf galaxies might be expected.

Simulations of the tidal 'harassment' in a Virgo cluster-like potential (Mastropietro et al. 2005) indicate that some galaxies can lose a significant fraction of their DM without much star loss, so that the remnant dwarf galaxy is dominated by stars in its inner region as we have found for the gap galaxies. An alternative possibility is that these low-mass dE galaxies were formed with little central DM. The gap galaxies may represent the first indication of a population of even lower mass dE galaxies that have similar dynamical masses to Local Group dSph galaxies but are star-dominated in their inner regions due to their location outside a giant galaxy halo. Dynamical studies of samples of low-mass dwarf galaxies, beyond the Local Group, with the next generation of large telescopes will be able to test this suggestion.

11 CONCLUSIONS

Using the ESI instrument on the Keck telescope, we have obtained internal kinematics for four dEs and one late-type dwarf galaxy. These galaxies were selected to have little, or no, nuclear component and indeed there is no evidence for a significant kinematically distinct nucleus in our data. The galaxies have K-band magnitudes down to $M_K \sim -17$ mag which places them in the 'gap' between previous dynamical mass measurements of dE galaxies by Geha et al. (2003) and Chilingarian (2009) and Local Group dSph galaxies and UCD objects located in the Virgo and Fornax clusters. We define the dynamical mass gap to be between $8 \times 10^7 < M_{\rm dyn}/{\rm M}_\odot < 5 \times 10^8$.

We measure central velocity dispersions of around 20 km s^{-1} for each galaxy. Supplemented by data from the literature for dE, dSph and UCD objects, we derive total stellar masses (mostly from K-band magnitudes) and dynamical masses (using the formulation of Wolf et al. 2010).

We find that the dE galaxies in the mass gap suggest a continuity from dE to dSph galaxies in terms of both their central velocity dispersion and effective radius with dynamical mass. This is also true when these systems are examined in the 3D space of the radius, dynamical mass and stellar mass. Such trends are qualitatively similar to those expected for dwarf galaxies from cosmological formation models. Interestingly, the dE galaxies in the gap reveal dynamical-to-stellar mass ratios, within their half-light radii, of unity. Thus, they appear to be stellar-dominated in their inner regions, similar to higher-mass dE galaxies and do not reveal the need for large DM fractions as inferred for Local Group dSph galaxies. We speculate that any DM in the inner regions of these low-mass dE galaxies has been 'puffed-up' to larger radii by gravitational heating effects from supernova feedback. Probing the dynamics of even lower mass dEs may reveal a population of dwarf galaxies that are dominated by stars in their inner regions.

ACKNOWLEDGMENTS

We thank J. Janz and T. Lisker for supplying their Virgo cluster dE data in a machine-readable form. We thank E. Tollerud and J. Wolf for useful discussions on galaxy scaling relations. This project made use of the NED and data products from the 2MASS, which is a joint project of the University of Massachusetts and the Infrared Processing and Analysis Center/California Institute of Technology, funded by the National Aeronautics and Space Administration (NASA) and the National Science Foundation. We thank the staff of the W. M. Keck Observatory for their support. Some of the data presented herein were obtained at the W.M. Keck Observatory, which is operated as a scientific partnership among the California Institute of Technology, the University of California and the NASA. We acknowledge financial support from the Access to Major Research Facilities Programme which is a component of the International Science Linkages Programme established under the

Australian Government's innovation statement, Backing Australia's Ability.

REFERENCES

Bagnulo S. et al., 2008, The ESO Messenger, 114, 10
Barazza F. D., Binggeli B., Jerjen H., 2003, A&A, 407, 121
Bekki K., Couch W. J., Drinkwater M. J., 2001, ApJ, 552, L105
Bender R., Burstein D., Faber S., 1992, ApJ, 399, 462
Benson A. J., Bower R., 2010, MNRAS, 405, 1573
Benson A., Frenk C., Lacey C., Baugh C., Cole S., 2002, MNRAS, 333, 177
Bertin G., Ciotti L., Del Principe M., 2002, A&A, 386, 149
Bovill M. S., Ricotti M., 2009, ApJ, 693, 1859
Brough S., Forbes D. A., Kilborn V. A., Couch W., Colless M., 2006, MNRAS, 369, 1351
Bruzual G., Charlot S., 2003, MNRAS, 344, 1000
Busarello G., Capaccioli M., Capozziello S., Longo G., Puddu E., 1997, A&A, 320, 415
Cappellari M., Emsellem E., 2004, PASP, 116, 138
Carter D., Sadler E., 1990, MNRAS, 245, 12
Chilingarian I. V., 2009, MNRAS, 394, 1229
Ciotti L., 1991, A&A, 249, 99
Ciotti L., Lanzoni B., 1997, A&A, 321, 724
Ciotti L., Lanzoni B., Renzini A., 1996, MNRAS, 282, 1
Collins M. L. M. et al., 2010, MNRAS, 407, 2411
Conroy C., Loeb A., Spergel D., 2010, ApJ, in press (arXiv:1010.5783)
Côté P. et al., 2006, ApJS, 165, 57
D'Onghia E., Besla G., Cox T. J., Hernquist L., 2009, Nat, 460, 605
Dabringhausen J., Hilker M., Kroupa P., 2008, MNRAS, 386, 864
De Rijcke S., Michielsen D., Dejonghe H., Zeilinger W. W., Hau G. K. T., 2005, A&A, 438, 491
De Rijcke S., Prugniel P., Simien F., Dejonghe H., 2006, MNRAS, 369, 1321
Djorgovski S., Davis M., 1987, ApJ, 313, 59
Djorgovski S., de Carvalho R., Han M.-S., 1988, Astron. Soc. Pac. Congress, 4, 329
Evstigneeva E. A., Gregg M. D., Drinkwater M. J., Hilker M., 2007, AJ, 133, 1722
Evstigneeva E. A. et al., 2008, AJ, 136, 461
Forbes D. A., Lasky P., Graham A. W., Spitler L., 2008, MNRAS, 389, 1924
Geha M., Guhathakurta P., van der Marel R. P., 2002, AJ, 124, 3073
Geha M., Guhathakurta P., van der Marel R. P., 2003, AJ, 126, 1794
Geha M., van der Marel R. P., Guhathakurta P., Gilbert K. M., Kalirai J., Kirby E. N., 2010, ApJ, 711, 361
Goerdt T., Moore B., Kazantzidis S., Kaufmann T., Macciò A. V., Stadel J., 2008, MNRAS, 385, 2136
Governato F. et al., 2010, Nat, 463, 203
Graham A., 2005, in Jerjen H., Binggeli B., eds, Proc. IAU Symp. 198, Near-field Cosmology with Dwarf Elliptical Galaxies. Kluwer, Dordrecht, p. 303
Graham A., Colless M., 1997, MNRAS, 287, 221
Graham A., Guzmán R., 2003, AJ, 125, 2936
Graham A., Guzmán R., 2004, in Block D. et al., eds, Penetrating Bars Through Masks of Cosmic Dust. Kluwer, Dordrecht, p. 723
Graham A., Worley C. C., 2008, MNRAS, 388, 1708
Graham A., Merritt D., Moore B., Diemand J., Terzić B., 2006, AJ, 132, 2711
Janz J., Lisker T., 2008, ApJ, 689, L25
Janz J., Lisker T., 2009, ApJ, 696, L102
Jerjen H., Binggeli B., Barazza F. D., 2004, AJ, 127, 771
Kalirai J. S. et al., 2010, ApJ, 711, 671
Kirby E. N., Guhathakurta P., Bolte M., Sneden C., Geha M. C., 2009, ApJ, 705, 328
Kroupa P., 1997, New Astron., 2, 139
Lane R. et al., 2010, MNRAS, 406, 2732
Lisker T., 2009, Astron. Nachr., 330, 1403
Macciò A. V., Kang X., Moore B., 2009, ApJ, 692, L109
Mamon G. A., Boué G., 2010, MNRAS, 401, 2433
Mashchenko S., Wadsley J., Couchman H. M. P., 2008, Sci, 319, 174
Mastropietro C., Moore B., Mayer L., Debattista V. P., Piffaretti R., Stadel J., 2005, MNRAS, 364, 607
Mayer L., Governato F., Colpi M., Moore B., Quinn T., Wadsley J., Stadel J., Lake G., 2001, ApJ, 559, 754
Mayer L., Kazantzidis S., Mastropietro C., Wadsley J., 2007, Nat, 445, 738
Mayer L., Kazantzidis S., Escala A., Callegari S., 2010, Nat, 466, 1082
Mei S. et al., 2007, ApJ, 655, 144
Mieske S. et al., 2008, A&A, 487, 921
Misgeld I., Hilker M., Mieske S., 2009, A&A, 496, 683
Montes D., Martin E. L., Fernandez-Figueroa M. J., Cornide M., de Castro E., 1997, A&AS, 123, 473
Moore B., 1996, ApJ, 461, L13
Moore B., Katz N., Lake G., Dressler A., Oemler A., 1996, Nat, 379, 613
Murray N., 2009, ApJ, 691, 946
Nagashima M., Yahagi H., Enoki M., Yoshii Y., Gouda N., 2005, ApJ, 634, 26
Navarro J. F. et al., 2004, MNRAS, 349, 1039
Okazaki T., Taniguchi Y., 2000, ApJ, 543, 149
Peñarrubia J., Navarro J. F., McConnachie A. W., 2008, ApJ, 673, 226
Prugniel P., Simien F., 1997, A&A, 321, 111
Romano-Diaz E., Shlosman I., Hoffman Y., Heller C., 2008, ApJ, 685, 105
Simien F., Prugniel Ph., 2002, A&A, 384, 371
Simonneau E., Prada F., 2004, Rev. Mex. Astron. Astrofís., 40, 69
Tollerud E., Bullock J., Graves G., Wolf J., 2011, ApJ, 726, 108
Toloba E., Boselli A., Cenarro A. J., Peletier R. F., Gorgas J., Gil de Paz A., Muñoz-Mateos J. C., 2011, A&A, 526, A114
Trentham N., Tully R. B., 2002, MNRAS, 335, 712
Trentham N., Tully R. B., Mahdavi A., 2006, MNRAS, 369, 1375
Valcke S., De Rijcke S., Dejonghe H., 2008, MNRAS, 389, 1111
Wolf J., Martinez G. D., Bullock J. S., Kaplinghat M., Geha M., Muñoz R. R., Simon J. D., Avedo F. F., 2010, MNRAS, 406, 1220
Zaritsky D., Gonzalez A., Zabludoff A., 2006, ApJ, 638, 725
Zaritsky D., Zabludoff A. I., Gonzalez A. H., 2008, ApJ, 682, 68
Zaritsky D., Zabludoff A., Gonzalez A., 2011, ApJ, 727, 116

This paper has been typeset from a TEX/LATEX file prepared by the author.